Characterization of Ordered 3D Arrays of Ag2S Nanocrystallites

L. Motte, F. Billoudet, D. Thiaudière, A. Naudon, M.-P. Pileni

Characterization of Ordered 3D Arrays of Ag_2S Nanocrystallites

L. Motte ([1,2]), F. Billoudet ([1]), D. Thiaudière ([3]), A. Naudon ([3]) and M.-P. Pileni ([1,2,*])

([1]) Laboratoire S R.S I. (**), Université P. et M. Curie (Paris VI), BP 52. 4 place Jussieu, 75231 Paris Cedex 05, France
([2]) C.E.A - C E.N Saclay, DRECAM., S.C M., 91191 Gif-sur-Yvette Cedex, France
([3]) Université de Poitiers, U.F.R Sciences, bâtiment SP2MI, Laboratoire de Métallurgie Physique (***), bd 3, Téléport 2, BP 179, 86960 Futuroscope Cedex, France

(Received 8 August 1996, revised 14 January 1997, accepted 20 January 1997)

PACS 68.65 +g – Low-dimensional structures (superlattices, quantum well structures, multilayers) structure and nonelectronic properties
PACS 61.46 +w – Clusters, nanoparticles and nanocrystalline materials
PACS.81 20.-n – Methods of materials synthesis and materials processing

Abstract. — Reverse micelles have been used to synthetize 5.6 nm silver sulfide particles. These nanoparticles are coated with dodecanethiol, extracted from reverse micelles and then dissolved in heptane The extracting process induces a size selection with a decrease in the polydispersity from 30% to 14%. By leaving a drop of a solution on any support, or immerse the support in the solution, mono and multilayers made of nanosized particles are formed The monolayer is arranged in a hexagonal network whereas the 3D multilayers are arranged in a face centered cubic structure. From T.E.M. (Transmission Electron Microscopy) and G.I.S A.X.S (Grazing Incidence Small Angle X-ray Scattering) techniques morphological information is provided

Résumé. — Dans cet article, la préparation et la caractérisation de réseaux ordonnés à deux et trois dimensions de nanocristallites de sulfure d'argent sont présentées. La morphologie des réseaux est étudiée à l'aide de deux techniques la microscopie électronique à transmission et la diffusion des rayons X aux petits angles sous incidence rasante. La microscopie électronique met en évidence un empilement de nanoparticules selon une structure cubique à faces centrées La distance moyenne entre particules et le nombre de couches formant la structure tridimensionnelle sont déterminés

Introduction

In the last decade a great effort has been devoted to control the size of nanoparticles [1]. Various colloidal methods as, reverse [2] and normal [3] micelles, Langmuir-Blodgett films [4], zeolite [5], two phases liquid-liquid system [6], organo-metallic techniques [7] and others, have been used

(*) Author for correspondence
(**) URA CNRS 1662
(***) URA CNRS 131

to control the size and polydispersity. In the range of 1 to 10 nm, unusual size dependence of the electronic properties of small metal [8–10] and semiconductor [11, 12] particles have been observed. It is necessary to control the size and reactivity of small particles to allow attachment of the particles to surfaces or to one another without leading to coalescence and hence loss of their size induced electronic properties. In all cases, surface passivation with coordinating ligand as alkanethiol [13, 14], alkyl phosphine [15] or dithiols [16], has been used to obtain a selection in size. This favors formation of particles which interact through strong attractive forces involving a larger energy than the thermal motion. This induces 2D and 3D ordered structures. This has been observed for semiconductors [13, 15] and gold particles [14, 16]. Such self assemblies should produce interesting properties such as new collective physical behavior. The development of a general procedure for the fabrication of quantum crystals is a major challenge of future research [17, 18].

In this paper, preparation and characterization of ordered 2D and 3D arrays made of Ag_2S nanocrystallites are presented. The study is focussed on particles having 5.6 nm as an average diameter Transmission Electron Microscopy, T.E.M., and Grazing incidence Small Angle X-ray Scattering, G.I S.A.X.S, are used to deduce the morphology of these aggregates. The 3D arrays are arranged in a face-centered cubic structure The average distance between particles and the number of layers forming the f.c.c structure are deduced.

1. Experimental Section

1 1. PRODUCTS. — Sodium di(2-ethylhexyl) sulfosuccinate usually called Na(AOT) was obtained from Sigma; isooctane from Fluka, sodium sulfide Na_2S from Janssen. Silver di(2-ethylhexyl) sulfosuccinate, Ag(AOT), was prepared as described previously [9].

1.2. APPARATUS

1.2.1 Transmission Electron Microscopy, T.E M. — The micrographs are obtained from JEOL 100CX operating at 100 kV. A drop of the solution is placed on a carbon film supported by a copper grid and the solvent is evaporated.

Histograms are obtained by measuring the diameter D_i of all the particles from different parts of the grid. About 500 particles are taking into account to establish the histogram. The standard deviation, σ, is calculated from the following equation:

$$\sigma = \left(\frac{\Sigma[n_i(D_i - D)^2]}{[N-1]} \right)^{1/2}$$

where D and N are the average diameter and the number of particles respectively.

1.2.2. Small Angle Scattering. — Small Angle X-ray Scattering, S.A.X.S., and Grazing Incidence Small angle X-ray Scattering, G.I.S.A.X.S, experiments [19, 20] were performed at the Laboratoire d'Utilisation du Rayonnement Électromagnetique (L.U.R.E , C.N.R.S.-C.E.A., Paris XI, Orsay, France) on the D22 diffractometer [21].

In Small Angle X-ray Scattering Experiments, S A.X.S., the scattered intensity is a function of the scattering angle, contrast, volume fraction, surface area, shape and size distribution of the scattering aggregates. The contrast is the electron density difference between the scattering aggregates and the surrounding matrix. Usually, S.A.X.S. is done in a transmission geometry. A new method in the scattering experiment is to align the sample in a grazing incidence geometry rather than in transmission one. This is the grazing incidence small angle X-ray scattering, G.I.S.A.X.S. The grazing incidence measurements were carried out by using a double-crystal monochromator, with two Ge (220) slabs. This selects a narrow energy

bandwidth ($\Delta E/E = 5 \times 10^{-4}$) in synchrotron beam emitted by the storage ring LURE-DCI running at 1.85 GeV. The beam was quasi-parallel to the horizontal plane. The chosen photon energy is 8049 eV, which corresponds to a wavelength of 1.54 Å. Two sets of horizontal and vertical slits were used to define a very narrow beam of 0.1 mm width in the vertical plane and 1 mm in the horizontal. The incident X-ray intensity was monitored by a NaI scintillator placed in front of the sample. The sample was set in the middle of a specially built cylindrical chamber [22] so that the sample could be aligned under the grazing incidence. The sample was positioned with its surface parallel to the X-ray beam. Two adjustments could be used for this: translation motion of the chamber and rotation of the sample. We considered the incidence angle α, to be equal to the zero ($\alpha = 0$ or the surface of the wafer is parallel to the X-ray beam) when the intensity of the incoming beam was reduced by 50%. The monochromator, slits and the chamber were all maintained in a vacuum of 1.3 torr with pipes connecting the different elements of the experimental set-up. The distance between the sample and the recording plane was at 650 mm. The scattering pattern of the sample was obtained with an Imaging-Plate (IP) detector. To analyze this two-dimensional image, cross sections will also be shown when discussing the following results.

1.2 3. S A.X S. and G.I.S A.X.S Treatments. — Assuming N particles, the scattered intensity $I(q)$ is

$$I(q) = N\ P(q)\ S(q) \tag{1}$$

where q is the wave vector and is equal to $4\pi(\sin\theta)/\lambda$ (2θ is the diffusion angle) and $P(q)$ and $S(q)$ are the form factor and the structure factor, respectively.

The form factor, $P(q)$, gives the average shape of the particles in 3D and 2D by S.A.X.S and G.I.S.A X.S., respectively

Because of the low volume fraction of Ag_2S particles dispersed in heptane (less than 0.01%), the structure factor, which takes into account the interactions between aggregates, can be assumed to be equal to unit. The scatter intensity is equal to the form factor.

The electron density of capped Ag_2S crystallites is higher than that of the particle surface HS ($C_{12}H_{24}$), formed by a dodecanethiol layer, and the scatter is due to spherical shells. The form factor is described by an inhomogeneous sphere model:

$$P(q) = [((\rho_s - \rho_{layer})v_{layer}B(q\ r_{layer})) + ((\rho_{layer} - \rho_{Ag_2S})v_{Ag_2S}B(q\ r_{Ag_2S}))]^2 \tag{2}$$

with

$$B(q\ r_i) = 3\left\{\frac{\sin q\ r_i - q\ r_i \cos q\ r_i}{(q\ r_i)^3}\right\}$$

where v_{Ag_2S} and r_{Ag_2S} are the volume and the radius of the particle without a layer and v_{layer} and r_{layer} are the volume and the radius of the particle surrounded by the layer formed by dodecanethiol ($C_{12}H_{24}SH$) at the particle surface. The electronic densities are fixed as $\rho_{layer} = 0.3\ e^-Å^{-3}$, $\rho_{Ag_2S} = 2.62\ e^-Å^{-3}$, and $\rho_s = 0\ 2\ e^-\ Å^{-3}$.

The thickness of the layer is defined as $r_{layer} - r_{Ag_2S} = 4$ Å.

The polydispersity in size has been estimated by assuming a Gaussian distribution. A root mean square deviation, σ, from the mean particle radius, $\langle r_{Ag_2S}\rangle$, broken brackets is deduced as previously described. From the Porod plot, $I(q)\ q^4$ *vs.* q, the characteristic diameter, D_c, is related to the first maximum and minimum of this representation by the following relationship:

$$D_c\ (\text{nm}) = \frac{0.54}{q_{max}} = \frac{0.9}{q_{min}}. \tag{3}$$

G I.S.A.X.S. is a recent surface analysis technique for the study of islands deposited on a flat surface. Consider the situation depicted in Figure 1, where a standard grazing incidence

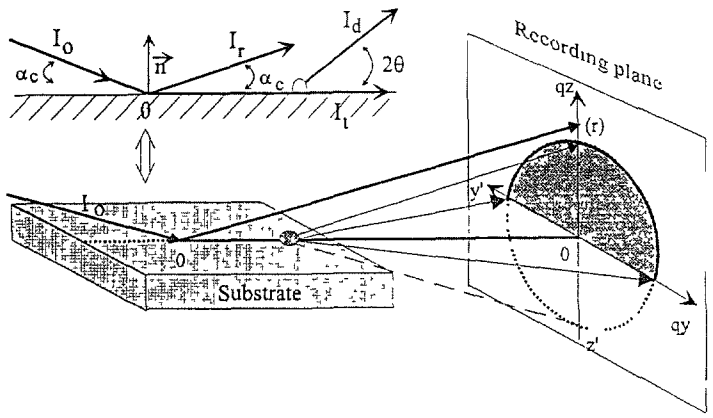

Fig. 1 — Scheme of the grazing incidence small angle X-ray scattering principle at critical angle.

geometry is shown. The incoming X-ray (I_0) encounters the surface of the substrate. When the incidence angle α is equal to the critical angle α_c of silicon ($\alpha_c = 0.22°$), a refracted beam (I_t) travels parallel to the surface and provides a considerably enhanced sensitivity. In fact, the refracted beam acts as a primary beam and consequently it gives a scattering signal (I_d) if there are aggregates on the surface. This is represented schematically by a dash area in the recording plane of the figure. The recording plane, indicated by the q_y- and q_z-axes, corresponds to a two dimensional detector (Imaging Plate for example). The momentum transfer q ($q = 4\pi(\sin\theta)/\lambda$) is equal to:

$$\mathbf{q} = \mathbf{q}_y + \mathbf{q}_z.$$

Moreover, the impact of the reflected beam I_r onto the image plate is represented by r. Just before the detector, a vertical beam-stop masks the strong intensity of the reflected beam. However, just only half of the scattering signal can be measured because the substrate avoids the lower scattering to be seen.

2. Results and Discussion

Sodium di(2-ethylhexyl) sulfosuccinate usually called Na(AOT) is used to form water in oil droplets called reverse micelles [23]. The water content, $w = [H_2O]/[AOT]$, is fixed to 20. This corresponds to an average droplet diameter equal to 6 nm [24]. Synthesis of Ag_2S nanocrystallites is performed by mixing two 0.1 M Na(AOT) micellar solutions: one contains 8×10^{-4} M of sodium sulfide, Na_2S, and the second one contains 8×10^{-4} M Ag(AOT) [9]. Due to Brownian motion, some collisions between droplets are efficient and the exchange process between water pools occurs. This favors the coprecipitation reaction between Ag^+ and S^{2-} ions. A few minutes after mixing the micellar solutions, silver sulfide, Ag_2S, nanosized particles are formed. Figure 2 shows the T.E.M. micrograph and histogram. The average diameter is 5 nm and the size distribution is closed to 30%.

Pure dodecanethiol is added to the reverse micellar solution containing Ag_2S nanocrystallites. After evaporation at 60 °C, the precipitate is washed with ethanol and filtered. The nanocrystallites coated by dodecanethiol are dispersed in heptane forming an optically clear solution.

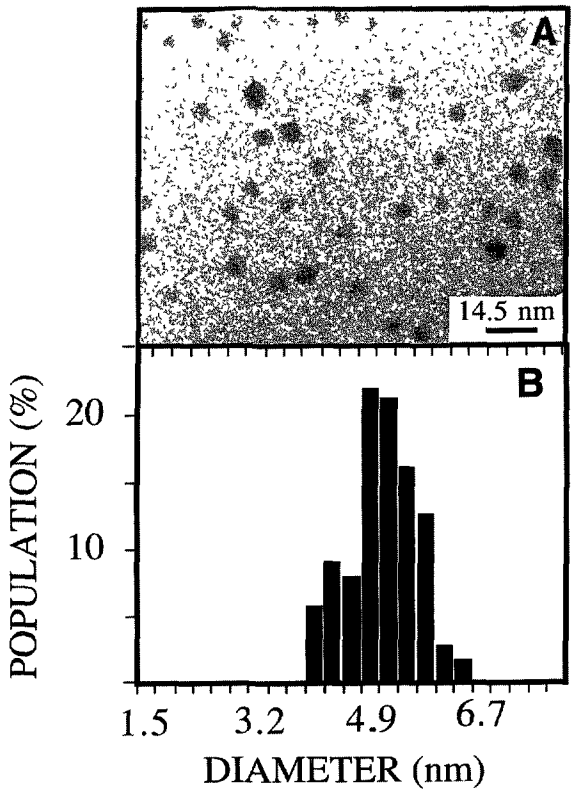

Fig 2 — Electron microscopy micrograph (A) and histogram (B) of Ag_2S particles made in reverse micelles at water content (w) equal to 20

The average size of the coated particles dispersed in heptane is determined from the maximum and minimum of the Porod Plot given in Figure 3. We found it to be equal to 5.8 nm and 5.5 nm respectively with 14% in polydispersity.

The T.E.M. micrograph obtained by evaporation of the diluted solution on a carbon grid shows the formation of a monolayer of particles on a very large domain (Fig. 4A). The histogram given in Figure 4B confirms an average particle size equal to 5.6 nm and the decrease in size distribution (14%) compared to that obtained in reverse micellar solution (Fig. 2). The T.E.M. micrograph shows that particles are ordered in monolayers forming hexagonal network (Fig. 4A). The average distance between particles is rather constant and is equal to 1.8 nm. It can be noticed that some parts of the carbon grid are not recovered by the monolayer (Fig. 4A).

When the carbon grid is left inside a concentrated solution made of Ag_2S particles, islands are formed in a very large domain (Fig. 5). Monolayers are still present in the T.E.M. micrograph. However in some part of the carbon grid, neither mono- nor multi-layers are observed. Enlarged view of an island, obtained in Figure 5, shows that it is formed by highly nanoparticles organized (Fig. 6A). High resolution of this island shows a high orientation of the particles in a four fold symmetry (Fig. 6B). This is attributed to orientation of the particles in the {001} plane of face centered cubic (f.c.c.) structure. As in a crystal, stacking defect in multilayer structure can be observed (Fig 6A). Furthermore, other organizations are also observed on the same T.E M micrograph. Figure 6C shows hexagonal symmetry, which corresponds to the stacking

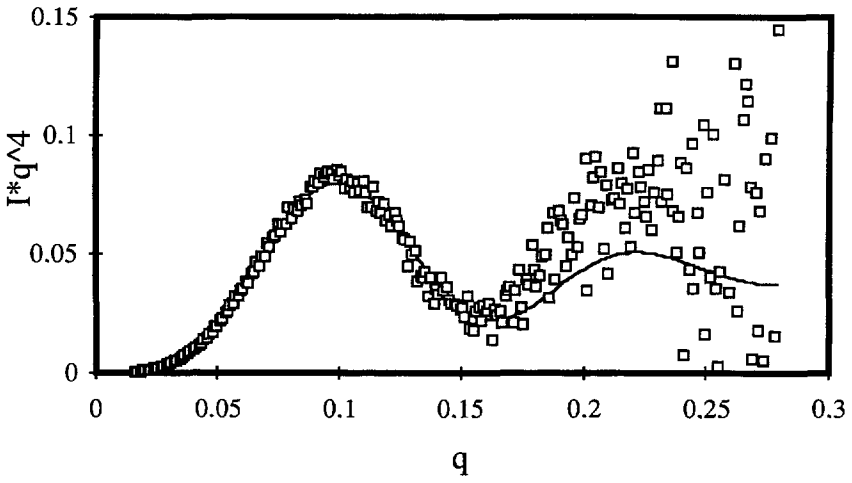

Fig 3. — Porod representations obtained from S.A X.S. experiments of silver sulfide particles dispersed in heptane (□) experimental data, (——) simulated curve

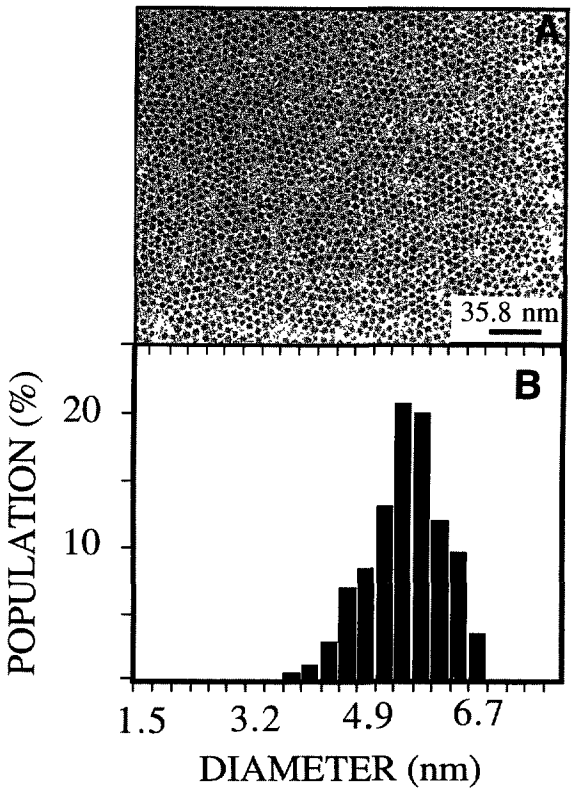

Fig 4 — T.E M micrograph of a monolayer of 5 6 nm Ag_2S particles (A) and its histogram (B)

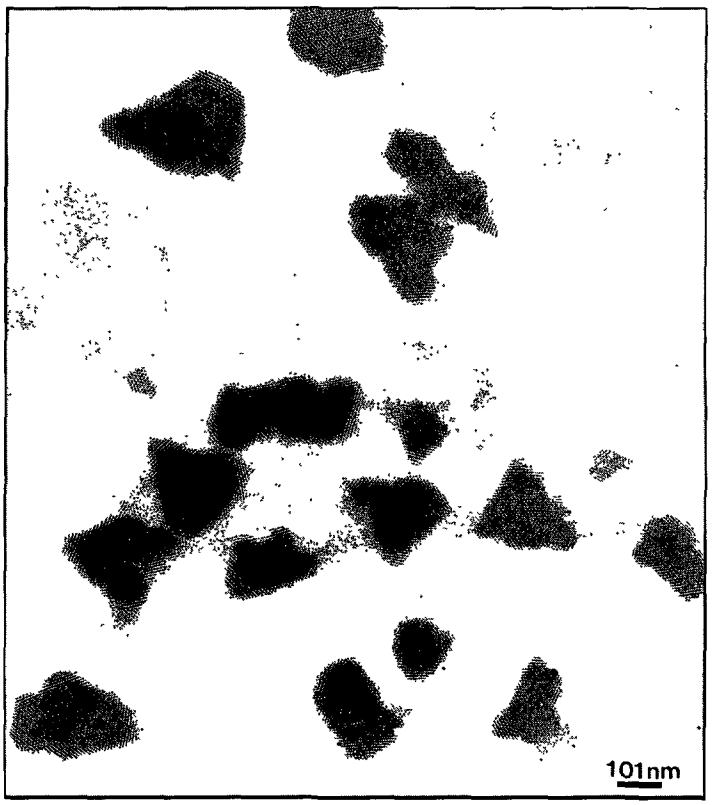

Fig. 5 — T.E M micrograph of particles obtained in a very large domain

of a {110} plane of the face centered cubic (f.c.c.) structure.

To study on a larger domain the mono- and multi-layers G.I.S.A.X.S. technique was performed. The solid support was a flat wafer and was immersed in the same experimental conditions (same solution) as the carbon grid used for T.E.M. micrograph and shown in Figure 5.

The scattering pattern (Fig. 7) shows two strong scattering streaks, symmetrical with respect to the vertical beam-stop. The weak streaks, observed along q_y and q_z axes, were second order scatter and indicate a high degree of organization of the aggregates in the planes parallel to the wafer surface. This is confirmed by the presence of the two strong streaks.

Figure 8A represents a cross section along q_y, for $q_z = 0$ The two main peaks of the 2D pattern are very sharp. That means the interference between aggregates is strong and indicates that the aggregates are very regularly distributed in the plane parallel to the wafer surface. According to T E.M. observations indicating a stacking of particles in a face centered cubic (f.c.c.) structure, the two main streaks correspond to {111} diffracting planes and the maximum in intensity observed in Figure 8A gives the mean distance between these planes:

$$d_{111} = \frac{2\pi}{q_A} = 8 \text{ nm}.$$

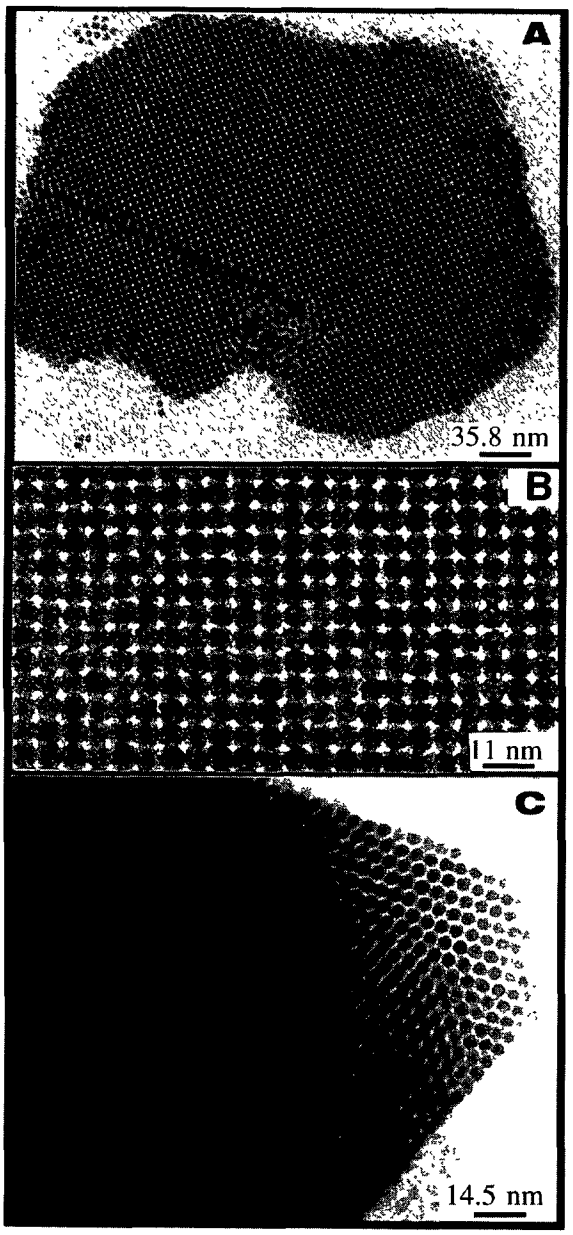

Fig. 6. — T.E.M micrograph of an island shown in Figure 5A, magnification of the island shown on A (B) and magnification of another island presented in Figure 5C

The mean inter-particle distance can be deduced and it is equal to·

$$\frac{2d_{111}}{\sqrt{3}} = 9.2 \text{ nm}.$$

Hence the mean distance between aggregates determined by T.E.M. and G.I.S.A.X.S. are found equal to 7.8 nm and 9.2 nm respectively. The difference between these two techniques can be

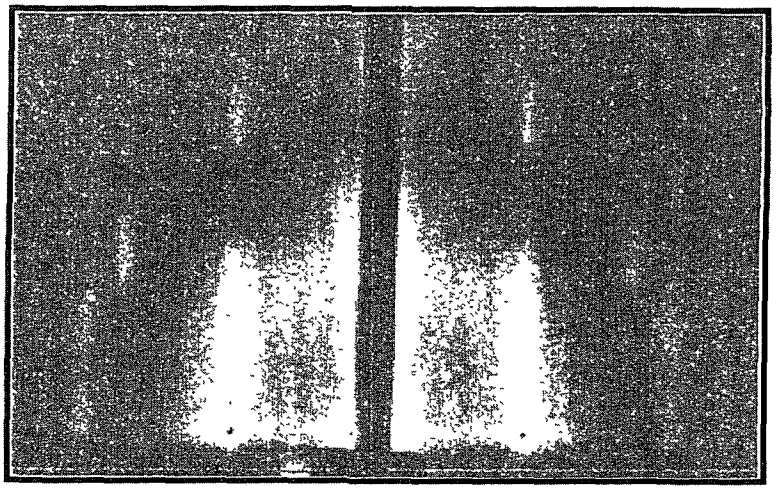

Fig. 7 — G I.S A X.S pattern of multilayers of Ag_2S particles.

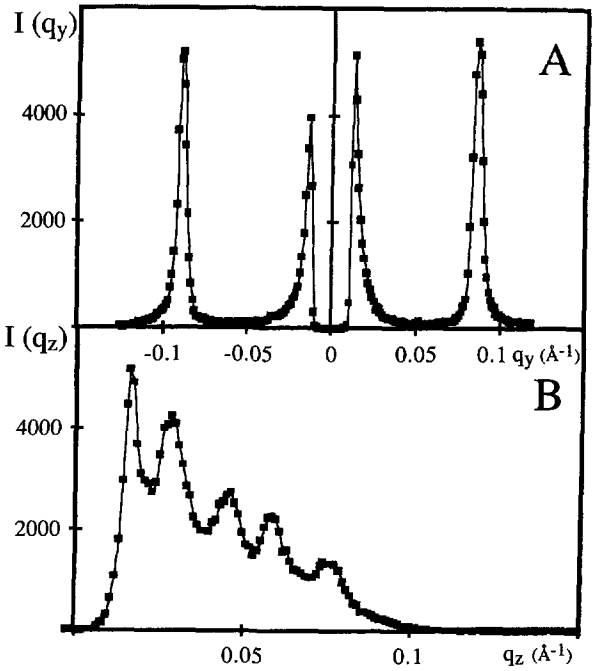

Fig. 8. — Cross sections of G I.S.A.X.S. pattern shown in Figure 7 along q_y (A) and q_z (B) axis

explained in term of the explored area: the T.E.M. micrograph shows organization of particles on a restricted area. The largest domain to measure the particle size and the inter-particle distance can be estimated to an area closed to 10^{-13} m^2. By using G.I.S.A.X.S. technique, the cross section of the X-ray beam is 10^{-6} m^2. Hence by G.I.S.A.X.S. the structural study is performed in a much larger domain compared to T.E.M. Figure 5 shows the presence of

zones which do not contain either mono- or multi-layers. It is reasonable to assume that similar behavior takes place on wafer support. Hence the absence of layer in some part of the solid support could explain the slight difference on the average distance between particles determined by T.E.M and G.I.S.A.X.S. and in the first approximation there seems to be a good agreement.

The cross section along q_z for $q_y = q\Lambda$ shows a regular oscillation of the intensity with q_z (Fig. 7C) This indicates that particles are also well ordered in the vertical direction over a large surface. These oscillations are the secondary maxima of a diffraction grating due to the stacking of several layers of Ag_2S monolayers. From the Δq_z distance between two maxima we found the total thickness T of the multilayer:

$$T = \frac{2\pi}{\Delta q_z} = 50 \text{ nm}.$$

This corresponds to an average of 7 layers of silver sulfide particles. Again because of the large domain of exploration by G.I.S.A.X.S., some of the supperlattices of silver sulfide are characterized by more than seven layers whereas others are formed by a smaller number of layer.

The envelope of the intensity along q_z corresponds to the mean form factor of the aggregates. It reaches zero for $q_z = 0.1$ Å^{-1}. Such a value gives 6 nm for the mean diameter of an aggregate. This data is a good agreement to that obtained by S.A.X.S. (Fig. 3) and by T.E.M. micrograph (Fig. 4)

Let us notice that in the vertical direction (along q_z) the structure factor $S(q)$ of equation (1) does not avoid the experimental determination of the size as for the horizontal direction; only a few aggregates are seen in the q_z direction

Conclusion

The present paper shows ordered three dimensional arrays of Ag_2S nanoparticles. They have been observed by using two complementary techniques: Transmission Electron Microscopy, T.E.M, and Grazing Incidence Small Angle X-ray Scattering, G I.S.A.X.S. By using T.E.M. a direct evidence of a stacking of 5.6 nm Ag_2S nanoparticles in a face-centered cubic structure is observed The average distance between particles is found equal to 7.8 nm Taking into account the 3D structure observed by TEM. the GISAXS technique gives quantitative average parameters on the number of layers and on the mean inter-particle distance. They are found equal to 7 layers and 9.8 nm, respectively. At large q angle, the average size of the particle is determined by G.I S.A.X.S. and S.A.X.S. This is in good correlation between these two measures. A good agreement between the T.E M and G.I.S.A.X.S techniques is obtained.

Acknowledgments

We wish to thank the technical staff of LURE-DCI for providing the synchroton beam and for assistance with the experiment.

References

[1] Clusters and Colloids, G. Schmid, Ed. (VCH Weinhem, 1994).
[2] Pileni M.P., Reverse micelles: a microreactor, *J. Phys. Chem.* **97** (1993) 6961

[3] Lisiecki I., Billoudet F. and Pileni M.P., Control of the shape and the size of copper metallic particles, *J. Phys. Chem.* **100** (1996) 4160.

[4] Fendler J.H. and Meldrum F.C., The colloid chemical approach to nanostructured materials, *Advanced Materials* **7** (1995) 607.

[5] Herron N., Wang Y., Eddy M., Stucky G.D., Cox D.E., Moller K. and Bein T., Structure and optical properties of CdS superclusters in zeolite hosts, *J Amer Chem. Soc.* **111** (1989) 530.

[6] Brust M., Walker D., Bethell D., Schiffrin D.J. and Whyman R., Synthesis of thiol-derivatised gold nanoparticles in a two-phase liquid-liquid system, *J. Chem. Soc. Chem. Commun.* **7** (1994) 801

[7] Murray C.B., Norris D.J. and Bawendi M.G., Synthesis and characterization of nearly monodisperse CdE (E = S, Se, Te) semiconductor nanocrystallites, *J. Am. Chem. Soc.* **115** (1993) 8706.

[8] Lisiecki I. and Pileni M.-P., Synthesis of copper metallic clusters by using reverse micelles as microreactors, *J. Amer. Chem. Soc.* **115** (1993) 3887.

[9] Petit C., Lixon P. and Pileni M.-P., Synthesis *in situ* of silver nanocluster in AOT reverse micelles, *J. Phys. Chem.* **97** (1993) 12974.

[10] Lisiecki I. and Pileni M.-P., Copper metallic particles synthesized *in situ* in reverse micelles: influence of various parameters on the size of the particles, *J. Phys. Chem.* **99** (1995) 5077

[11] Brus L.E., A simple model for the ionization potential, electron affinity, and aqueous redox potentials of small semiconductor crystallites, *J. Chem. Phys.* **79** (1983) 5566.

[12] Rossetti R , Ellison J.L., Bigson J.M. and Brus L.E., Electron-electron and electron-hole interactions in small semiconductor crystallites· the size dependence of the lowest excited electronic state, *J. Chem. Phys.* **80** (1984) 4464.

[13] Motte L , Billoudet F. and Pileni M.-P., Self assembled monolayer of nanosized particles differing by their sizes, *J. Phys. Chem.* **99** (1995) 16425.

[14] Ohara P.C., Leff D.V., Heath J R. and Gelbart W.M., Crystallization of opals from polydisperse nanoparticles, *Phys. Rev. Lett.* **75** (1995) 3466.

[15] Murray C.B., Kagan C.R. and Bawendi M G., Self-organization of CdSe nanocrystallites into three-dimensional quantum dot superlattices, *Science* **270** (1995) 1335.

[16] Brust M., Bethell D., Schiffin D.J. and Kiely C.J., Novel gold-dithiol nano-networks with non-metallic electronic properties, *Adv. Mater.* **9** (1995) 797

[17] Heath J.R., The chemistry of size and order on the nanometer scale, *Science* **270** (1995) 1315.

[18] Heitmam D. and Kotthaus J.P., The spectroscopy of quantum dot array, *Phys. Today* **6** (1993) 56.

[19] Naudon A., Slimani T. and Goudeau P., Grazing small-angle scattering of X-rays for the study of thin surface layers, *J. Appl. Cryst.* **24** (1991) 501.

[20] Levine J.R., Cohen J.B., Chung Y.W. and Georgopoulos P., Grazing-incidence small-angle X-ray scattering: new tool for studying thin film growth, *J. Appl. Cryst.* **22** (1989) 528.

[21] Dubuisson J.M., Dauvergne J.M., Depautex C., Vachette P. and Williams C.E., *Nucl. Instrum. Methods A* **246** (1986) 636.

[22] Naudon A. and Thiaudiere D., Determination of the morphology of deposited islands by grazing incidence small angle X-ray scattering, *Surface and Coating Technology* **79** (1996) 103.

[23] Structure and Reactivity in Reverse Micelles, Pileni M.-P., Ed. (Elsevier, Amsterdam, 1989).

[24] Pileni M.-P., Zemb T. and Petit C., Solubilization by reverse micelles: solute localization and structure perturbation, *Chem Phys. Lett.* **118** (1985) 414.